https://doi.org/10.5194/egusphere-2022-644
Preprint. Discussion started: 20 July 2022

Seismic Characteristics of the Largest Measured Subglacial Flood from the Eastern Skaftá cauldron, Iceland

Eva P. S. Eibl[1], Kristin S. Vogfjörd[2], Benedikt G. Ófeigsson[2], Matthew J. Roberts[2], Christopher J. Bean[3], Morgan T. Jones[4], and Bergur H. Bergsson[2]

[1]University of Potsdam, Institute of Geosciences, Karl-Liebknecht-Str. 24-25, 14476 Potsdam, Germany
[2]Icelandic Meteorological Office, Bústaðavegi 7–9, 108 Reykjavík, Iceland
[3]Geophysics Section, School of Cosmic Physics, Dublin Institute for Advanced Studies, 5 Merrion Square, Dublin 2, Ireland
[4]Center for Earth Evolution and Dynamics (CEED), University of Oslo, PO Box 1028, Blindern 0315 Oslo, Norway

Correspondence: Eva Eibl (eva.eibl@uni-potsdam.de)

Abstract. Subglacial floods are hazardous events. Since seismic tremor accompanies them, the source can be located and tracked in space and time using a seismic array. However, understanding how these seismic signals are generated remains elusive. Here, we study the seismic characteristics of the largest measured flood from the Eastern Skaftá cauldron, Iceland. We track the propagation of the flood in 2015 using two seismic arrays and a local seismic network. Data from three GPS instruments above the cauldron lake and the subglacial flood path and from hydrological instruments in the Skaftá river aid the interpretation. We find that as the water drained from the lake, quakes were generated in the area around the cauldron and the glacier surface subsided by more than 100 m. We detected several-hours-long, non-harmonic tremor migrating downglacier following the subglacial flood front. We suggest that this tremor is composed of repeated, closely spaced icequakes generated as the glacier was being lifted, cracked and deformed enabling the subglacial water flow. When the lake had largely drained, we recorded minute-long tremor bursts with hour-long harmonic tails emanating from the cauldron area. Body waves compose the bursts. We interpret them as hydrothermal explosions in the geothermal system underlying the cauldron, followed by vigorous boiling due to the pressure drop within the hydrothermal system as a consequence of the lowering of the water level in the lake. We conclude that the three different tremor characteristics are associated with three different geophysical processes.

1 Introduction

Subglacial volcanic and geothermal systems beneath glaciers cause a substantial flood hazard to areas surrounding glaciers (Waythomas et al., 2013; Björnsson, 2003; Magnússon et al., 2012; Roberts, 2005; Cook et al., 2018; Eibl et al., 2020). Glacial outburst floods, termed jökulhlaups in Icelandic, can occur through steady melting above ice-covered geothermal areas (Björnsson, 2003, 2010), through melting by magma–ice interaction during a volcanic eruption (Björnsson, 2003; Gudmundsson et al., 1997; Sturkell et al., 2008), as well as through the release of water stored in subglacial or marginal lakes dammed by glaciers

https://doi.org/10.5194/egusphere-2022-644
Preprint. Discussion started: 20 July 2022

(Björnsson, 1976; Roberts et al., 2005; Bartholomaus et al., 2015; Grinsted et al., 2017; Lindner et al., 2020; Livingstone et al., 2019; Behm et al., 2020) or moraines (Cook et al., 2018). Improving the understanding of source processes and generation mechanisms of subglacial floods is challenging as (i) the flood has to be detected beneath several hundred meters of ice; (ii) instruments are either difficult to maintain on the ice and nunataks within the ice or they are located outside the glacier, far from the signal generating source; and (iii) seismic signals accompanying a flood are often weak, non-impulsive, long-lasting, lack discernible seismic phases and are therefore intrinsically difficult to analyse for source location and mechanism.

In close proximity of rivers it has been found that long-lasting seismic signals referred to as tremor, are generated both by turbulent flow and bedload transport in rivers (Burtin et al., 2011; Gimbert et al., 2014, 2016; Schmandt et al., 2013). The tremor amplitude correlates with the discharge (Hsu et al., 2011; Burtin et al., 2008) as was recently confirmed in a glacial environment (Bartholomaus et al., 2015; Gimbert et al., 2016). Bartholomaus et al. (2015) correlate the tremor amplitude at 1.5 to 10 Hz measured at 1 to 5 km distance with the discharge. Gimbert et al. (2016) explain the tremor amplitude between 2 to 12 Hz as due to turbulent flow interacting with the bed roughness. However, they suggest that at more than 1 km distance, the seismic noise caused by turbulent water flow dominates over the noise caused by bedload transport.

At larger distances the seismic signal linked to turbulent water flow still needs to be distinguished from other possible tremor sources. There are a variety of interpretations for the generating tremor source in a glacial environment (Podolskiy and Walter, 2016) including resonating water filled cracks or channels (Röösli et al., 2014; Chapp et al., 2005; Winberry et al., 2009; Heeszel et al., 2014; Lindner et al., 2020), englacial water flow in a moulin (Röösli et al., 2014, 2016; Lindner et al., 2020), regularly repeating icequakes (MacAyeal et al., 2008; Winberry et al., 2013; Müller et al., 2005; Lindner et al., 2020; Behm et al., 2020) and hydrothermal boiling (Leet, 1988; Montanaro et al., 2016). When studying the propagation and mechanisms of subglacial floods, these different sources need to be characterised and distinguished from flood-related water flow. However, despite various reports on seismic signals such as quakes and tremor before and during subglacial floods (Winberry et al., 2009; Bartholomaus et al., 2015; Lindner et al., 2020; Behm et al., 2020), a thorough and continuous tracking of the flood migration beneath the ice from the draining lake to the glacier terminus was only recently achieved by Eibl et al. (2020) for 4 subglacial floods in Iceland. At 10 to 52 km distance they detect a migrating tremor source with peak frequency at 1.3 Hz.

Iceland is an ideal place to study subglacial flood-related seismic signals as there are multiple subglacial floods per year that produce detectable signals such as tremor (Eibl et al., 2020). In several glaciological, geomorphological or hydrological studies (Böðvarsson et al., 1999; Einarsson, 2009; Einarsson et al., 2016; Old et al., 2005; Roberts et al., 2003), filtered one-minute averages of the seismic signal are used to exhibit the evolution and characteristics of different jökulhlaups. These filtered signals suggest that the seismic character of subglacial floods changes with time, where in particular floods draining subglacial high-temperature geothermal areas exhibit the following characteristics: a periods of quakes, intermixed with or followed by weak tremor that is followed by strong tremor bursts. If no network stations are located near the flood path, then the weak tremor is usually not detected above the background noise. Due to a lack of continuous data, sparse seismic networks and uncertainties in the timing of the subglacial propagation of these floods, there has so far been little in-depth, seismological analysis of this type of activity and the processes that might generate it.

In 2013 we installed a multidisciplinary network that was (i) specifically installed to monitor subglacial floods from west

https://doi.org/10.5194/egusphere-2022-644
Preprint. Discussion started: 20 July 2022

Vatnajökull, and (ii) used to demonstrate a real-time early-warning capability. Eibl et al. (2020) mainly focused on the weak tremor accompanying the subglacially migrating flood for more than 17 h. This study tracked four subglacial floods with peak discharges in the range of 210 to 3000 m^3/s using one seismic array (a cluster of closely spaced sensors capable of resolving direction to the tremor source and the apparent speed of the waves across the array) outside the glacier. They derived subglacial propagation speeds for all the floods and concluded that seismic arrays can be used to detect the floods several hours in advance of the hydrological network in the area outside the glacier margin, allowing an improved early-warning.

Using the same array in conjunction with the SIL national seismic network, GPS, hydrological and geochemical data (section 3), here we provide a detailed analysis of the various seismic signals caused by one of the largest measured jökulhlaups in Iceland. It occurred in September–October 2015 originating from the eastern Skaftá cauldron in the west Vatnajökull ice cap (section 4.1). We describe the quakes (section 4.2), weak persistent tremor (section 4.3) and strong tremor bursts (section 4.4) in detail. We discuss the flood initiation (section 5.1), the tremor generation during the flood propagation in the context of the known flood path (section 5.2.1) and the tremor generation in the cauldron area in the context of the pressure drop (section 5.2.2). Finally, we put the propagation speed of the flood into a global context (section 5.3) and conclude that the tremor exhibits three different characteristics associated with different geophysical processes.

2 The Skaftá Cauldrons

Localized geothermal melting of ice at the base of a glacier causes the formation of a depression in the glacier surface, often surrounded by cylindrically symmetric crevasse patterns. The depression leads to a decrease in ice-overburden pressure and consequently forces geothermal meltwater, geothermal fluids, percolating rain water, and surface meltwater to accumulate beneath the cauldron. Water accumulates as a subglacial lake until the water pressure is close to the ice-overburden pressure at the location of the weakest seal near the edge of the lake. The lake drains rapidly after outflow begins through the seal (Björnsson, 1977, 1988, 2003).

Two subglacial lakes in the western part of Vatnajökull ice cap, southeastern Iceland, 10 and 15 km WNW of Grímsvötn volcano, are the source of regular jökulhlaups in the Skaftá river (Fig. 1) (Björnsson, 2003; Jóhannesson et al., 2007). The eastern and western cauldron each have a width of 1–3 km, depth of 50–150 m and host ca. 100 m deep subglacial lakes at their highest stage shortly before jökulhlaups are released (Jóhannesson et al., 2007). Combined, they drain approximately 65 km^2 of the ice cap (Pálsson et al., 2014). Finite-element ice-flow calculations show that ice-surface depressions caused by the emptying of the subglacial lakes are considerably larger than the footprint of the corresponding water body at the glacier bed (Einarsson et al., 2017).

Jökulhlaups from the Skaftá cauldrons into the Skaftá river catchment have been observed since 1955 (Zóphóníasson, 2002; Björnsson, 1977; Þórarinsson and Rist, 1955). Floods earlier than 1955 may have taken alternate drainage pathways outside the ice margin into Langisjór lake without leading to noticeable floods in the river course further downstream (Björnsson, 1977; Tómasson and Vilmundardóttir, 1967). The jökulhlaups occur every 1 to 5 years from each cauldron with volumes of 0.05 to 0.4 km^3 and maximum discharge rates of 50 to 3000 m^3/s (Björnsson, 1977, 1992; Zóphóníasson, 2002). The locations of the

https://doi.org/10.5194/egusphere-2022-644
Preprint. Discussion started: 20 July 2022

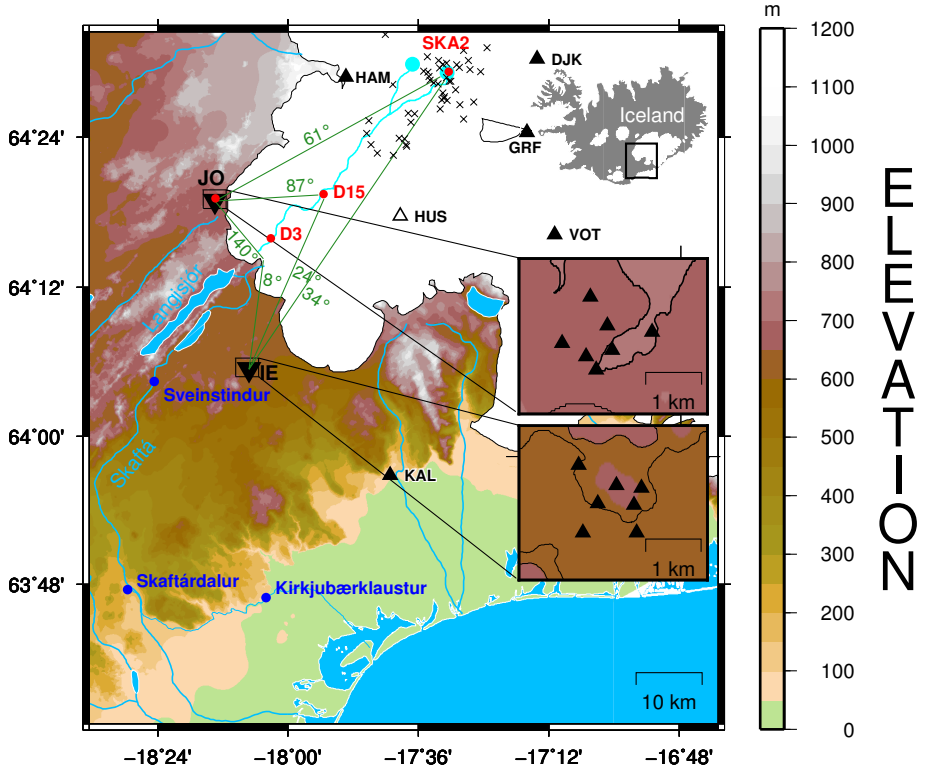

Figure 1. Instrument network on and west of Vatnajökull ice cap monitoring the 2015 jökulhlaup in Skaftá river. The eastern and western cauldrons (cyan dots) and subglacial and subaerial flood path (cyan line) (Björnsson, 1986, 1988) are marked. The locations of Jökulheimar (JO) and Innri-Eyrar (IE) seismic arrays (inverted black triangles), single seismic stations (black triangles, open if not working during the jökulhlaup), the GPS instruments (red dots) and hydrological stations (blue dots) are indicated. Locations of quakes are marked with black ×-signs and back azimuths from JO and IE with green lines with numbers. The insets show (top) an overview of Iceland with glaciers marked in white, (middle) geometry of the JO array and (bottom) geometry of the IE array.

flood paths were estimated based on the gradient of the hydraulic potential derived from radio-echo sounding studies of the ice thickness and bedrock topography beneath the ice (Björnsson, 1986, 1988). The geometry of the hydraulic potential based on the radio-echo sounding measurements and the observed outlet locations of jökulhlaups at the ice margin of Skaftárjökull outlet glacier indicate that the location of the subglacial flood path shown in Fig. 1 has remained the same since jökulhlaups in Skaftá were first reported in the 1950s.

https://doi.org/10.5194/egusphere-2022-644
Preprint. Discussion started: 20 July 2022

3 Methods

3.1 Seismic Processing

The seismic signals generated by the flood were recorded using two seismic arrays with an aperture of 1.6 km (black inverted triangles in Fig. 1) and the Icelandic Meteorological Office's (IMO) national seismic network, SIL (Böðvarsson et al., 1996; Böðvarsson and Lund, 2003) (black triangles in Fig. 1).

In the Vatnajökull region, the SIL network consists of broadband (Güralp 3ESPC 60s and 120s, Güralp 6T Flutes 10s, Trillium Compact 20s, Geotech KS2000 100s) and short period (Lennartz 5s) stations, some installed on nunataks and within the ice. This network monitored the seismic activity associated with the flood. The closest stations DJK, HAM and GRF at 13–15 km distance from the draining cauldron recorded both quakes and tremor, but event locations, which mostly relied on P- and S-wave arrivals on the 3 to 7 closest stations, were hampered by emergent onsets, small magnitudes and low signal/noise ratios as well as station failures (HUS and horizontal components of DJK) and frequent earthquakes from Bárðarbunga volcano following its eruption in 2014/15 (Sigmundsson et al., 2014). As a result only a few events were located by the automatic SIL system. A review of the seismic network records, as part of this study, has enabled location and magnitude determination of 45 events near the cauldron and the flood path (Fig. 1) between 28 September and 2 October, using the SIL analysis software and velocity model (Rögnvaldsson and Slunga, 1993; Stefansson et al., 1993). Hypocentral location uncertainties are, however, rather large, up to 2–4 km in some cases.

The telemetered arrays, specifically installed to record subglacial floods, consist of seven stations (six 3-component Güralp 6TDs (10 s to 100 Hz) and one 3-component Güralp 3ESPCD (60 s to 50 Hz)) at Jökulheimar (JO, centered at the SIL station JOK) and Innri-Eyrar (IE) southwest of Vatnajökull at 38–52 km distance from the cauldron (5L seismic network, (Bean and Vogfjörd, 2020)). During a flood, they can be used to locate and track the emergent, long-lasting, low amplitude tremor. As preprocessing steps we detrend, instrument-correct and down-sample the recordings to 20 Hz and divide them into 1 h long time windows. At the JO array, local noise sources dominate around 1 Hz while the flood–related signal was strongest around 1.3 Hz and clearly detectable above the noise. Our analysis and interpretation here is mainly based on the results from one array (JO) and the a priori knowledge of the subglacial flood path.

We performed a frequency–wavenumber analysis using the vertical component of the signal filtered between 1.2 and 2.6 Hz with a moving 18 s long time window as described in Capon (2009) and implemented in Beyreuther et al. (2010) and Megies et al. (2011). A grid search for maximum power was carried out in a horizontal slowness grid with a stepsize of 0.02 s/km and limits of $\pm$1.0 s/km. The resulting time series (Fig. 3d and e) contain back azimuth and slowness, which reflect the direction and steepness of the dominant incoming wave, respectively. At less than 50 km source–receiver distance, migrating subglacial flood-related tremor sources can be tracked with high temporal and spatial resolution, and changes in tremor source depth or wavetype can be detected. Time windows with a semblance of less than 0.3 were discarded.

The uncertainty in the back azimuth and slowness estimates based on the array geometry, is estimated using the width of the peak in the array response function in the horizontal slowness grid: We determine back azimuth and slownesses of all points that have a power of at least 95% of the maximum (Eibl et al., 2017b). We discard points with an uncertainty in back azimuth

https://doi.org/10.5194/egusphere-2022-644
Preprint. Discussion started: 20 July 2022

greater than 12° and uncertainty in slowness greater than 0.2 s/km. The resulting mean uncertainty for each back azimuth or slowness estimate was 4.2° and 3.0° in back azimuth and 0.04 s/km and 0.03 s/km in slowness at JO and IE array, respectively. When binning back azimuth estimates over a longer time period it becomes apparent whether the tremor is emitted at a spatially confined location, as indicated by little variation in the back azimuth with time, or whether the tremor source comprises a larger region, as indicated by scattering in the back azimuth with time.

We used the 45 quakes that were located using the SIL network to test our arrays for a systematic bias in back azimuth for signals coming from that direction and depth. The source locations were used to calculate expected back azimuths at the JO and IE arrays. Performing array processing on these events we could compare expected back azimuths and array–located back azimuths. Due to a low signal-to-noise ratio, only 17 events could be used at the JO array and 12 events at the IE array. For these earthquakes, the array–determined back azimuths were on average 9.3° too low at the JO and 10.1° too high at the IE array. It is likely that the back azimuths are systematically shifted due to heterogenities in the seismic velocity structure under W-Vatnajökull related to volcanic ridges striking north-northeast–south-southwestwards beneath the ice cap. We keep this in mind when discussing potential tremor source locations as this systematic shift may be expected to affect tremor sources as well if they originate in the same region. Squinting arrays with systematic offsets between the actual source and array back azimuths were reported in (Eibl et al., 2017a; Krueger and Weber, 1992; Schweitzer, 2001).

To additionally assess the tremor amplitude, we calculated the Root Median Square (RMeS) of the seismic recordings (Fig. 3c): The data were instrument-corrected, detrended, tapered and filtered between 1.0 and 2.0 Hz. The vertical component of the velocity seismogram of one seismometer in each array was divided into 60-minute long time windows and RMeS was calculated. The time window was then shifted, allowing 75% overlap. Calculating RMeS instead of RMS strengthens the tremor signal while giving less weight to shorter transients such as earthquakes (Eibl et al., 2017b). To assess the spectral characteristics of the seismograms and enhance the continuous signals in the tremor, spectrograms were created using window lengths of 64 to 256 s and overlap of 50–70%.

3.2 GPS and Hydrological Measurements

A streaming Trimble NetRS GPS instrument was installed by the IMO near the center of the eastern cauldron (SKA2) from July 2014 to October 2015 for early-warning purposes. Two additional identical GPS instruments were installed above the subglacial flood path on the glacier at 15 and 3 km distance from the ice terminus (D15 and D3, respectively, Fig. 1 and Einarsson et al. (2016)). Mainly D15 was used to constrain the travel time of the subglacial jökulhlaup. Instrument D3 was washed away when a small part of the flood water hydrofractured through the ice. However, it was found the following summer on the surface of the glacier. Data were recovered from the internal memory card and used to constrain the speed of the subglacial flood wave, although the data do not contain information about the movement of the ice during the flood at this location. The GPS data were processed using the GAMIT-Track utility (Herring et al., 2015) with the continuous GPS station at JOKU in Jökulheimar as base (Fig. 3a).

Hydrological data of the Skaftá river were obtained from IMO's pressure-sensor stage meters at Sveinstindur, 28 km down-

https://doi.org/10.5194/egusphere-2022-644
Preprint. Discussion started: 20 July 2022

stream from the glacier margin, and Skaftárdalur, 40 km downstream from Sveinstindur (Fig. 1) and include the river level, electric conductivity and water temperature (Fig. 3b). The river level was used to calculate flood discharge using a rating curve.

4 Results and Interpretation

4.1 Propagation of the Subglacial Flood According to GPS and Hydrological Measurements

Based on the GPS and hydrological instruments, the flood started to propagate in the early hours of 30 September, reached D15 at 17:30 of the same day and the hydrological station 25 km downstream at 4:00 on 1 October (Eibl et al., 2020). However, the GPS instrument SKA2 already recorded a slow subsidence from noon on 27 September (Fig. 3a). Slowly increasing outflow of water from the subglacial lake on the order of a few cubic meters per second started at this time but the water was stored subglacially near the cauldron for about 3 days.

The subglacial lake emptied rapidly and the 300 m thick ice-shelf dropped by approximately 60 m in 24 hours. The subsidence of SKA2 on top of the ice-shelf slowed down rather abruptly at a lowering of about 66 m, accelerated again and fell by another 17 m by 3 October (Fig. 3a). It should be noted that at the end of the subsidence the GPS instrument was not located at the deepest part of the cauldron. Mapping of the ice-surface geometry of the cauldron after the jökulhlaup showed two deep pits lowering by up to 40 m more than that at the center, probably caused by local maxima in the geothermal heat flux at geothermal vents at the glacier bottom, which melt large domes into the bottom of the ice-shelf. The continued slower subsidence recorded by the GPS instrument may have been caused by the local collapse of such thinner areas of the ice-shelf.

The flood started to lift the overlying ice at D15 for one day, reaching a maximum of approximately 1 m at 16:00 on 1 October (Fig. 3a). The flood was accompanied by an order of magnitude increase in horizontal velocity of the glacier to 1–2 m/d. The glacier surface then subsided over a two day period back to the level before the jökulhlaup. While the subsidence hovered around 66 m, the flood lifted D15 to its maximum height.

The D3 instrument detected no changes in glacier motion before midnight on 30 September. The flood must, therefore, have arrived later at this location, 3 km from the ice terminus. As river stage and conductivity rapidly increased from 04:00 on 1 October (Fig. 3b), the flood front most likely reached the ice terminus between 01:00 and 02:00 and fractured the ice at several locations 1–3 km from the terminus. These outbreaks were marked by up to 3–5 m high and 10 m wide ice fragments on the surface of the glacier, alongside debris deposited from the floodwater (see Fig. 2). Towards the ice terminus the fragments decreased in size, down to a few centimeters or tens of centimeters in diameter near the ice margin. After the first pulse, water continued to flow beneath the ice to outlets at the margin.

4.2 Flood Initiation and Quakes Recorded on Closest Seismic Stations (SIL)

Seismic records from HAM and DJK, the stations closest to the draining cauldron, show that the onset of cauldron subsidence and slow outflow of water on 27 September did not immediately trigger seismic activity in the cauldron area. The first located event occurs 16 hours later in the early hours of 28 September, within 4 km distance west of the cauldron center (Fig. 1 and

https://doi.org/10.5194/egusphere-2022-644
Preprint. Discussion started: 20 July 2022

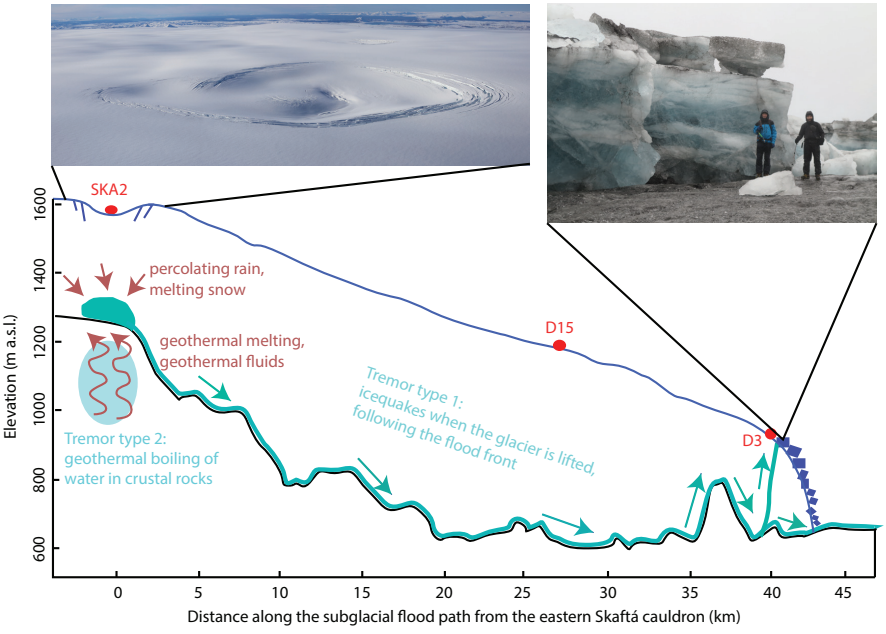

Figure 2. Schematic diagram along the subglacial flood path from the eastern Skaftá cauldron based on figure 3.6 in Einarsson (2009) and figure 2 in Jóhannesson et al. (2007). The photos show (left) an aerial view of the eastern Skaftá cauldron from the east after the September/October 2015 jökulhlaup. The western cauldron can be seen in the distance to the right of the center of the image. Semi-circular crevasses mark the boundary of the area that subsided. Thrust ridges due to inward ice flow have formed near the center of the depression during the 10 days that had elapsed since the flood to the time when the photo was taken. Photo: Oddur Sigurðsson, 10 October 2015. (right) Large ice blocks broken from the glacier surface by the initial outburst flood through the glacier at 3 km distance from the ice margin. Photo: Tómas Jóhannesson, 1 October 2015.

3c). Only two events of M 0.7 were located that day in the cauldron area and another two smaller events in the afternoon and evening of the following day. On 30 September when the cauldron subsidence started accelerating, the seismic activity also escalated, to well over 100 events/hour in the afternoon (Fig. 4a and b).

However, because of the small magnitudes and overlapping signals, only 12 events could be located. Five of them were south-west of the cauldron area, along or in the vicinity of the subglacial flood path. The location of the first such event, 13 km from the cauldron at 11:03 on 30 September supports the inference from the GPS and hydrological data that the flood front had started propagating from the cauldron area around 04 in the morning. The high seismic activity continued into 1 October, when the cauldron subsidence was the fastest, until around 14:00 when both seismicity and rate of subsidence swiftly decreased. In this period, another 19 events could be located, of which 7 were along or near the flood path. As the seismicity decreased, signs of tremor bursts appeared – the first one at 12:15 on 1 October – and continued through 2 October when they were the dominant activity on the seismic records. During this final phase, 10 additional events were located in the cauldron area and two along or near the flood path.

https://doi.org/10.5194/egusphere-2022-644
Preprint. Discussion started: 20 July 2022

A total of 45 seismic events were located in the cauldron area, mostly within 4 km distance from the center, and along or near the upper part of the subglacial flood path (Fig. 1). Their source depths locate predominantly near the surface, with 33 events within 1 km from the surface. Event magnitudes range from ML 0 to ML 1.6. No events were located along the lower half of the subglacial flood path. Due to the emergent event onsets and small signal/noise ratios, the event locations have considerable uncertainty. However, they mostly cluster within the expected source areas and the recorded signals show the expected characteristics of shallow source depth and propagation in the near surface, which result in long P and S wavetrains and dominance of low frequencies (Vogfjörd and Langston, 1996). The duration of signals on the array stations is around 30–35 seconds (Fig. 5c) and the frequency content above background from 1–8 Hz for the smallest events and 1–15 Hz for the largest. Dominant frequencies were at 1–3 Hz.

Due to their short duration with respect to the length of the moving time window in the array analysis, they do not affect the calculated back azimuth of the tremor.

4.3 Seismic Tremor Related to the Advancing Subglacial Flood Front (Type 1)

Eibl et al. (2020) found that the subglacial flood was accompanied by a migrating tremor source (Type 1). However, we would like here to point out the details of the migrating tremor source. While the flood front arrived at D15 at ca. 17:30 on 30 September (Fig. 3a), stronger Type 1 tremor started at 18:40 (Fig. 4) in an area about 1 km farther downstream (Fig. 4). D15 reached its maximum elevation about 20 h later, the strongest tremor came from a location farther south and became weak on the last 8 km of the subglacial flood path. Along the whole flood path, Type 1 tremor was strongest in regions of adverse bedrock slope (up-slope flow about 35 kilometers down the flood path, see Fig. 2) and close to the ice terminus (Fig. 3a and d). The back azimuth first reached 140° at 01:30 on 1 October. This strong tremor close to the ice terminus might be linked to the hydrofracturing of the ice that happened about 3 km upstream from the ice terminus. However, the tremor near the terminus was also exceptionally strong from 01:30 to 02:45 and 03:35 to 04:09 on 1 October (Fig. 4b and c). In general, we can conclude that Type 1 tremor was generated in an area spanning up to 20° as measured from JO array that migrated downglacier with time.

The black line in Fig. 4c shows the back azimuth corresponding to a point migrating along the flood path at 2 km/h that crosses D15 at 17:30 on 30 September. It aids the visual interpretation of the tremor back azimuths, as this curve shows how the location and shape of the flood path map into changes of the back azimuth with time. It indicates that most of the tremor back azimuth is consistent with source locations upstream of a migrating flood front with a rather constant propagation speed near 2 km/h. Tremor is further generated in an elongated area as tremor is visible for up to 12 hours at some locations.

4.4 Tremor Bursts from the Cauldron (Type 2)

(Eibl et al., 2020) detected Type 2 tremor bursts from 16:00 on 1 October on JO and IE arrays. On the closest stations from the SIL network (e.g. GRF), a tremor band around 2 Hz was detected from 09:30 on 1 October. A first weak tremor pulse was detected at noon (Fig. 3d and e, Fig. 6, Fig. 7). Type 2 tremor stopped at 22:00 on 2 October when the ice-shelf had almost fully subsided.

https://doi.org/10.5194/egusphere-2022-644
Preprint. Discussion started: 20 July 2022

In detail, Type 2 tremor started with an emergent, up to 15 minutes long burst (Fig. 7) with a frequency content up to 7 Hz. The burst was followed by an up to 6 hour long harmonic tail with an overtone spacing of about 0.2 Hz (Fig. 7). The fundamental frequency is not visible due to low-frequency noise. The first and last bursts (including their tails) were weaker while the strongest and longest started at 01:00, 11:00 and 14:00 on 2 October before the last phase in the settling of the ice-shelf started around 16:00.

We isolated the back azimuths of Type 2 tremor (Fig. 8a and b) and created histograms with 2° wide bins (Fig. 8c and d). The grey bars in Fig. 8a and b indicate the uncertainty associated with every back azimuth estimate based on the array geometry (see Methods). The median back azimuth ± standard deviation during all tremor bursts were 53.1±15.6° at JO and 50.1±16.6° at IE. The large standard deviation/ scatter of these values indicates that Type 2 tremor was generated over a wide region.

Given that slownesses indicate a Type 2 tremor source in the bedrock (Eibl et al., 2020) and that back azimuths roughly point towards the eastern cauldron, they might be generated in roughly the same region as the quakes. For these quakes, we determined back azimuths that are 10.1° too large at IE and 9.3° too low at JO array. If the tremor back azimuths are affected similarly, Type 2 tremor was in reality generated at an average back azimuth of 62.4° from JO and 40.0° from IE. This corresponds approximately to the area of the cauldron (see Fig. 1).

5 Discussion

5.1 Triggering of the Flood

The cauldron subsidence, as recorded by the GPS instrument on top of the subglacial lake, started on 27 September 2015. The first quake appeared about 16 h later and seismic activity peaked when the cauldron subsidence sped up and the flood propagation started. Therefore, no seismic activity in form of earthquakes or icequakes was detected when the seal failed. This failure led to an initial slow water loss from the subglacial lake, which only a few days later developed into a flood wave migrating downhill.

In contrast, a flood in 2016 from a glacier-dammed, marginal lake on Glacier de la Plaine Morte, Switzerland was presumably triggered by icequakes (Lindner et al., 2020). When the melt season started and progressed Lindner et al. (2020) were able to track how an efficient draining system progressed upglacier. Since they recorded icequake signals near the lake basin in the 24 h period before the lake drained, they suggest that hydrofracturing linked the ice-dammed marginal lake to this drainage system and led to a flood. Here, at the Skaftá cauldrons such hydrofracturing might not be a relevant flood trigger, since the lake is located at the bedrock-ice interface and therefore does not cause vertical hydrostatic pressure aiding a hydrofracturing event.

The quakes recorded here are interpreted as a sign of brittle failure. They are located near the bedrock-ice interface and we cannot differentiate whether they originated in the ice or bedrock. They appear once the water started to slowly migrate from the subglacial lake and might therefore be caused by the pressure change induced in the bedrock. Alternatively these quakes could be signs of further failure of the seal or linked to the subsidence of the ice layer, opening crevasses that are visible on the

https://doi.org/10.5194/egusphere-2022-644
Preprint. Discussion started: 20 July 2022

surface (Fig. 2). These quakes potentially caused by crevasses are clearly distinguishable from the various tremor sources due to a higher frequency content.

5.2 Tremor Generation in General

Due to a variety of potential source processes and several studies of seismic tremor in glacial environments (see review in Podolskiy and Walter (2016)), various tremor models coexist. These can be broadly grouped in several categories based on the suggested source mechanism. Tremor is interpreted as resonance in a subglacial water-filled crack or conduit (Chapp et al., 2005; Winberry et al., 2009) or generated by englacial water flow (Röösli et al., 2014), linked to fluid-flow-induced vibrations in grounded icebergs (Müller et al., 2005), drag of turbulent water against the bed roughness (Bartholomaus et al., 2015), repeating icequakes (MacAyeal et al., 2008; Lipovsky and Dunham, 2016) or hydrothermal boiling (Leet, 1988).

5.2.1 Flood-related Tremor Generation (Type 1)

For the Skaftá 2015 jökulhlaup, the subglacial Type 1 tremor source moved gradually southwards accompanying the subglacial propagation of the flood. Based on the geometry of the flood path, we calculated the back azimuths we would expect from a flood front propagating at constant speed along the path (see section 4.3 and Fig. 4). The back azimuths of the Type 1 tremor closely followed these expected back azimuths of the flood front during the flood. Tremor was furthermore generated in a long migrating region and was strongest in regions with adverse bedrock slope. As plausible tremor models we consider turbulent flow, impact during bedload transport, resonance and repeating icequakes.

Resonance might be triggered by water flow in a subglacial channel (Müller et al., 2005) or between the bedrock and ice layer. However, if resonance is triggered in this manner we would expect tremor generation along the whole flood path, not mainly following the propagating flood front. In addition, the strong tremor in regions of adverse slope cannot be explained by this model.

If tremor were induced by turbulent flow, we would expect a high tremor amplitude along the entire flood path upstream of the flood front. Instead, we find that the tremor source moved and started for example at the GPS instrument D15 shortly after the first sign of the flood was detected there. The tremor amplitude is highest while the glacier is being lifted, especially in regions of adverse bedrock slope, and the tremor source moves southwards following the flood front. Additionally, we detected differences in tremor generation along the flood path with little tremor on the upper half of the flood path. As we expect similar water flow speeds and turbulence along the whole flood path upstream of the flood front, our observations are not consistent with tremor generation by turbulent flow.

Our surface wave observation, however, is consistent with the Rayleigh wave-dominated glaciohydraulic tremor reported by Vore et al. (2019) at more than 1 km distance from the source. Lindner et al. (2020) recorded tremor before and during a flood at the Glacier de la Plaine Morte, Switzerland and interpret them as signs of ice fracturing, moulins and moulin resonance that hide potential tremor linked to turbulent flow. Lindner et al. (2020) did not manage to track the propagating flood front, but

https://doi.org/10.5194/egusphere-2022-644
Preprint. Discussion started: 20 July 2022

located a persistent tremor source near an outlet and interpret it as linked to subglacial water flow. This might be consistent with our observation that tremor is strongest near the outlet and on the lowermost part of the flood path. However, for Skaftá floods we were far from the source (>50 km) and it remains to be shown whether tremor signals along the flood path have varying amplitude or whether the signal amplitude was merely modulated by the distance between the flood and array location.

Tremor caused by bedload sediment transport is thought to be characterised by a frequency content of more than 9 Hz while pressure fluctuations in turbulent flow is thought to be characterised by a frequency content of less than 9 Hz (Bartholomaus et al., 2015; Gimbert et al., 2016). These observations are made a few kilometers from the source and at larger distances the high frequencies will be attenuated. At 10 to 52 km distance, we observe tremor that is strongest around 1.3 Hz. The bedload transport studies indicate that bedload sediment transport is not a likely source generation in the present case. The Skaftá floods might in addition transport little sediment in comparison to other sites globally, as mentioned by Bartholomaus et al. (2015); Gimbert et al. (2016); Cook et al. (2018).

We suggest that the Type 1 tremor was generated by the high strain rates caused by the advancing water front. The glacier is lifted quickly up to 1 m off the bedrock and hence behaves in an elastic way in contrast to its usual plastic behaviour. The water front can flow into these newly formed cracks and propagate them further. This lifting is inferred to be typical for the front of fast-rising jökulhlaups (Jóhannesson, 2002; Björnsson, 2010; Einarsson et al., 2016, 2017; Magnússon et al., 2007). The area of increased velocity was studied with InSAR during a flood in 1995 and found to be at least 9 km wide (Fig. 6 in (Magnússon et al., 2007)). This mechanism implies that the ice underwent brittle fracturing that resulted in small, repeated, closely spaced icequakes that could merge into tremor as suggested by MacAyeal et al. (2008) for colliding icebergs. This process may be assumed to have been particularly intense at the tip of the flood front at each point in time but continued until the discharge reached the maximum at each location. According to this interpretation, the first strong tremor period around 02:00 on 1 October from the direction of the glacier terminus might be due to the hydrofracturing of the ice that is likely to have been especially intense as the flood lifted the thinner ice near the terminus. While most of the water continued to flow near the bedrock, tremor might have decreased after the hydrofracture reached the surface. The second stronger tremor period (around 04:00 on 1 October) most likely marks further ice fracturing as the flood discharge near the terminus increased. In addition, the seismic sources generated in a lifted ice sheet might not couple well to the ground once the ice sheet is separated by the water layer.

Similarly, Behm et al. (2020) recorded a rapidly-rising jökulhlaup in Zackenberg river in Greenland that was accompanied by intense surface crevassing as inferred from seismic icequake detection by seismometers on the ice. They suggest that increased basal sliding leads to increasing seismicity and crevassing on the surface. We are most likely too far from the source to detect these icequakes caused by the ice movement. However, we speculate that during the flood when parts of the ice cap speeds up, crevassing and seismicity intensifies. This might merge into what we record as non-harmonic tremor at more than 10 km distance due to scattering effects of the shallow bedrock layers (Ying et al., 2015). A GPR study in Greenland also detected basal crevassing (Behm et al., 2020), that might be similar to the hydrofracture we observed here, which here ruptured all the

https://doi.org/10.5194/egusphere-2022-644
Preprint. Discussion started: 20 July 2022

way to the ice surface near the terminus.

The migrating tremor source is spread over up to 20° along the flood path as seen from the JO array. This indicates that tremor does not start immediately when the flood front arrives but that the ice surface needs to be lifted further before tremor becomes visible from each location. In the context of tremor that is composed of icequakes, this suggests that a threshold number of icequakes are required before tremor is detected at our observational range. The width of the flood front, ∼9 km as derived from InSAR studies (Magnússon et al., 2007), may also be expected to contribute to the spread of the calculated back azimuth. The activated region is therefore large and icequakes are likely neither similar enough nor spaced regularly enough to generate harmonic tremor such as observed during strike-slip collisions of edges of icebergs MacAyeal et al. (2008). Large-scale sliding events of a glacier in Antarctica, not associated with a subglacial flood, were accompanied by tremor episodes at the ice–bed interface. They were interpreted as repeating earthquakes due to the clear presence of single events and harmonic character of the observed gliding tremor (Lipovsky and Dunham, 2016). Tremor in our case neither shows harmonic character nor clearly repeating events that might compose it. The visible peaks in the seismogram of Fig. 4a are linked to the quakes around the eastern cauldron or other volcanically active regions. Additionally, our GPS recordings indicate that the glacier is lifted up to 1 m off the bedrock which led us to conclude that tremor might be generated by irregularily repeating icequakes while ice is hydrofractured rather than earthquakes on fault planes on the bedrock-ice interface.

We observe a substantial but short-lived increase in horizontal velocity of the glacier at each GPS location when the pressure wave passes (Einarsson et al., 2016). The maximum of the velocity increase coincides with the maximum of lifting and decreases as the wave has passed by. The velocity increase is partly due to shear thinning but mostly due to increase basal sliding of the glacier. Both increased scraping at the bottom of the ice or stick-slip motion could lead to tremor generation. This would then follow the location of the flood front and would not be detected once the flood reaches the glacial river. This is consistent with the Type 1 tremor locations that stopped at the glacier terminus.

While other glacier-seismology studies (Bartholomaus et al., 2015; Lindner et al., 2020) report a tight correlation between discharge and tremor amplitude in the 1 to 10 Hz band, Eibl et al. (2020) do not report a correlating diurnal variation but rather a temporal offset in tremor amplitude and discharge. However, floods with larger peak discharge are still accompanied by larger tremor. The time offset might be caused by large distances between instruments or due to flow of water between the ice and bedrock in a wide area instead of a channelized flow (Eibl et al., 2020).

Nevertheless, we note that Type 1 tremor still continues to increase in amplitude after the flood front has reached the terminus of the glacier and has the highest amplitude early on 2 October for the 2015 flood. This tremor might be formed by the subglacial water flow. This interpretation is able to explain the following points: i) its magnitude follows the discharge on 1 October, ii) it seems to be generated along the whole flood path as seen by seismic signals that are not coming from only one specific direction, iii) it should be more distinct for the large flood from the eastern cauldron than for the small floods from the western cauldron as observed by Eibl et al. (2020).

If a GPS instrument measures a pronounced lifting of the ice this indicates that the capacity of the subglacial drainage system was overwhelmed by the abrupt water escape (Lindner et al., 2020). For example, Lindner et al. (2020) report a peak discharge

https://doi.org/10.5194/egusphere-2022-644
Preprint. Discussion started: 20 July 2022

and GPS/ ice lifting in the first hours when the moulin reached the lake bottom. Consequently, the GPS elevation lowered to levels before the drainage, the discharge measured in the river dropped, while the lake drained slower and incised into the ice to drain through the moulin. In this study, the GPS is lifted even more in a second pulse and the peak discharge is only measured 4 days after slow outflow from the lake was detected. The draining water overwhelmed the capacities of the subglacial drainage system leading to a pronounced ice lifting and widespread flow of water beneath it.

5.2.2 Cauldron Tremor Generation (Type 2)

Taking bias in the back azimuth from the JO and IE arrays into account, back azimuths during Type 2 tremor point towards an area near the eastern cauldron (compare Fig. 1 and Fig. 8).

While (Eibl et al., 2020) report on harmonic Type 2 tremor, here we observe further spectral details. We observed about ten pulses. Each of these tremor pulses starts with an emergent burst and is followed by an hour-long harmonic tail. Similarly, Montanaro et al. (2016) reported 40 to 50 s long explosions with frequency content up to 4 Hz followed by a several minute long tail of elevated tremor during a flood from a semi-subaerial lake at Kverkfjöll, N-Vatnajökull, in 2013. They suggest explosions due to expansion of boiling fluid in the geothermal reservoir followed by vigorous boiling. Remnants of such explosions were observed from the air the following day. This observation was the first time such a subglacial tremor burst could be confirmed visually. While they reported a drop of 30 m at Kverkfjöll, we observed more than 100 m at the Skaftá cauldron and hence a larger pressure decrease that might cause the long tremor duration reported here.

The temperature in the subglacial geothermal area may be assumed to be close to the pressure boiling point of water except at shallow depths near the glacier bed (e.g. Gudmundsson and Björnsson (1991); Ármannsson (2016). This implies that a lowering of the overlying pressure by ∼0.6–1 MPa, corresponding to a drop in water level of ∼60 m as well as the lowering of the effective pressure in the lake due to bridging stresses in the subsiding ice shelf (Einarsson et al., 2017), will lead to a lowering of the pressure boiling point within the geothermal system in the range 5–15 K (Wagner et al., 2000). A lowering of the pressure boiling point of this magnitude will lead to vigorous hydrothermal boiling of water in shallow crustal rocks, which explains the creation of body waves by this tremor source.

Small volcanic eruptions are not likely to be the cause of Type 2 tremor, as water samples showed elevated concentrations of dissolved inorganic carbon (DIC) and major elements including Ca, Mg, and B (see supplementary material for details on geochemical data). High DIC concentrations are indicative of sustained water–rock interaction prior to subaerial exposure, and peak concentrations during this flood are comparable to previous floods from the Skaftá cauldrons (Jones et al., 2015; Galeczka et al., 2015). Boron is a strong indicator of geothermal activity given its high mobility (Arnórsson and Andrésdóttir, 1995). The boron concentration peaked at 18.3 μmol/L in the pro-glacial river at Kirkjubæjarklaustur. This is over 4 times higher than measurements from the 2014 flood from the western Skaftá cauldron at the same locality (Jones et al., 2015), indicating that the non-glacial-melt part of the floodwater is of geothermal origin that has taken years to accumulate.

The geothermal chemical signature of the water suggests that the reservoir built up gradually beneath the ice cap, with continued and long-lasting reactions with the bed rock. However, this gradual process is aseismic and a migrating seismic signal only begins after the flood commenced (Eibl et al., 2020).

https://doi.org/10.5194/egusphere-2022-644
Preprint. Discussion started: 20 July 2022

5.3 Speed of Floods Globally

(Eibl et al., 2020) combined GPS, hydrological and seismic data to estimate the speed of the flood. They derive an average speed of 2 km/h (0.6 m/s) for the lowermost 15 km of the flood path from GPS and hydrological measurements and an average speed of 1.4–2.4 km/h (0.4–0.7 m/s) along the flood path from seismic observations. Assuming constant speed upstream of D15, the timing derived for the start of the flood from near the cauldron at 04 on 30 September is in broad accordance with the time when the rate of cauldron subsidence started to accelerate.

We calculated the expected back azimuths along the known flood path and converted the distance along the flood path to time assuming a constant velocity of 2 km/h as discussed above (Fig. 4). The resulting change in back azimuth with time closely fits the initiation of Type 1 tremor observed at each location along the path, indicating (i) approximately constant flood propagation along the path and (ii) less bias in back azimuth for Type 1 tremor generated at or above the ice–rock interface along the flood path than Type 2 tremor generated at depth in the crust. We might expect less bias in the back azimuth for Type 1 tremor composed of surface waves traveling in the glacier ice, as ice is more homogeneous than volcanic bedrock. The Type 2 tremor interpreted to be generated at depth in the crust is sensitive to possible heterogenities in the seismic velocity structure of the crust. A strong Type 1 tremor source that we interpret as an area of substantial lifting somewhat upstream of the flood front clearly moved downglacier from an area near the cauldron to the glacier margin (Fig. 6). Exact estimates of the initial arrival of Type 1 tremor or the time of maximum tremor intensity at specific locations of the flood path are hard to derive because of the wide scatter in the data.

On the lowermost part of the flood path (D15 to the glacier margin) the average change in the back azimuth at the JO array may roughly correspond to flood front propagation of ∼15 km in 6–7 hours, in crude agreement with propagation estimated from GPS and hydrological data. The variation of the back azimuth from higher up the path to the glacier margin is harder to estimate because the Type 1 tremor signal from the upper part of the path is weak. It does not allow us to make a statement on how the propagation speed varies as the flood moves through the glacier.

The flood in September/ October 2015 propagated faster than other known jökulhlaups in Iceland. In October 1995, Magnússon et al. (2007) found that on the last 7 km of the subglacial flood path the speed of the flood front during a small jökulhlaup from the eastern cauldron was less than 0.06 m/s (0.2 km/h). This is an order of magnitude lower than the average speed we derive during the jökulhlaup in 2015, but Magnússon et al. (2007) described the flood in 1995 as an unusually small one, occurring unexpectedly only 3 months after a large jökulhlaup from the same cauldron. Einarsson et al. (2016) and Einarsson et al. (2017) report subglacial flood propagation speeds of 0.2–0.4, 0.1–0.3 and 0.4–0.6 m/s for jökulhlaups from the western cauldron in September 2006 and August 2008 and from the eastern cauldron in October 2008, respectively. Similarly, Eibl et al. (2020) report propagating speeds in the range of 0.2 and 0.4 m/s (0.9-1.6 km/h, 0.7-1.1 km/h and 0.8-1.3 km/h) for three subglacial floods from the western Skaftá cauldron. These differences might be caused by the flood size as Eibl et al. (2020) conclude that floods with a smaller peak discharge propagate slower.

Larger velocities were derived on other glaciers in Iceland and worldwide. A large jökulhlaup from Grímsvötn, Iceland, in 1996 propagated at 5 km/h (Björnsson, 2003; Jóhannesson, 2002). Benediktsdóttir et al. (2021) calculated subglacial flood

https://doi.org/10.5194/egusphere-2022-644
Preprint. Discussion started: 20 July 2022

speeds during the Eyjafjallajökull eruption 2010 of 2.0, 2.5, 3.75 and 15 km/h for floods of similar size as we reported here. The propagation speed of subglacial floods in other glaciers worldwide have been reported as 6.1 m/s (22 km/h) for glaciers in the Pacific northwest (Richardson, 1968) and >2 m/s (>7.2 km/h) (Driedger and Fountain, 1989) at Mt. Rainier in Washington state in the US and >1.05 m/s (3.8 km/h) in Switzerland (Werder and Funk, 2009). Larger speeds might be due to larger flood sizes (Eibl et al., 2020), a larger gradient of the topography or other factors that are not constrained in detail yet.

6 Conclusions

The September/October 2015 jökulhlaup in the Skaftá river was one of the largest measured floods in Iceland since the start of hydrological measurements at Sveinstindur in 1971. The flood was released after an unusually long interval of more than five years since the previous jökulhlaup from the eastern Skaftá cauldron. This subglacial flood in Iceland was accompanied by a characteristic seismic sequence consisting of (i) a few second long quakes, (ii) hour-long non-harmonic Type 1 tremor and (iii) approximately 10 to 15 minutes long Type 2 tremor bursts followed by an up to 6 hour-long harmonic tail. We suggest that the source of the Type 1 tremor observed during the subglacial propagation of the Skaftá jökulhlaup is repeating icequakes generated while the ice is quickly forced upwards to allow water flow below. The elevation of the ice surface increased for up to 1 day. Type 2 tremor bursts were interpreted as hydrothermal explosions in the cauldron area and their harmonic tail as vigorous boiling. Type 2 tremor bursts and their tail indicate the drainage of floodwater from the cauldron and the associated lowering of water pressure in the subglacial geothermal system, respectively.

Globally most studies report on quakes (Behm et al., 2020) or tremor (Winberry et al., 2009; Bartholomaus et al., 2015; Lindner et al., 2020; Vore et al., 2019) during floods. Iceland however seems to be a unique place where fast rising jökulhlaups may be followed by tremor bursts potentially caused by the active geothermal system driven by the active subglacial volcanic systems. Despite geothermal activity in Greenland or Antarctica (Fahnestock et al., 2001; Loose et al., 2018; Schroeder et al., 2014) a similar sequence of seismic signals remains to be reported in other regions with volcano-ice interaction. The methods described and knowledge gained here can aid in the identification of flood signals and their differentiation from eruption–related signals in other glacier-covered, volcanically active regions worldwide that can lead to hazardous flooding.

Code and data availability. Seismic data are available via GEOFON (5L seismic network, (Bean and Vogfjörd, 2020)). The array processing was performed using the freely available Python toolbox ObsPy.

Author contributions. EE., CB. and KV. initiated the study conception and design. Data collection was performed and supported by BB., EE., BO., MR. and MJ.. Data analysis was performed by EE., KV., BO. and MJ. The first manuscript draft was written by EE. and all authors commented on previous versions of the manuscript. All authors read and approved the final manuscript.

https://doi.org/10.5194/egusphere-2022-644
Preprint. Discussion started: 20 July 2022

Competing interests. There are no competing interests.

Acknowledgements. Field work, data collection and analysis was performed within the framework of FutureVolc, funded by the European Union's Seventh Programme for research, technological development and demonstration under grant agreement No. 308377. MTJ is supported by the Research Council of Norway (project numbers 223272 and 263000). We thank Bergur Einarsson for fruitful discussions, Martin Möllhoff, Heiko Buxel, Baldur Bergsson, Vilhjálmur S. Kjartansson and Þorsteinn Jónsson for technical support and Aoife Braiden for support in the field. Water samples were collected at Skaftárdalur and Kirkjubæjarklaustur by IMO staff. We acknowledge the assistance of Tómas Jóhannesson in providing data and contributing to the interpretation presented in the paper. We extend our thanks to Iwona Galeczka for processing of these samples at the University of Iceland.

The Landsvirkjun (National Power Company of Iceland) Research Fund, the Icelandic Road Administration, the Kvískerja fund and the Iceland Glaciological Society have supported the glaciological field work and research on jökulhlaups from the Skaftá cauldrons.

https://doi.org/10.5194/egusphere-2022-644
Preprint. Discussion started: 20 July 2022

References

Ármannsson, H.: The fluid geochemistry of Icelandic high temperature geothermal areas, Applied Geochemistry, 66, 14–64, https://doi.org/10.1016/j.apgeochem.2015.10.008, 2016.

Arnórsson, S. and Andrésdóttir, A.: Processes controlling the distribution of boron and chlorine in natural waters in Iceland, Geochimica et Cosmochimica Acta, 59, 4125–4146, https://doi.org/10.1016/0016-7037(95)00278-8, 1995.

Bartholomaus, T. C., Amundson, J. M., Walter, J. I., O'Neel, S., West, M. E., and Larsen, C. F.: Subglacial discharge at tidewater glaciers revealed by seismic tremor, Geophysical Research Letters, 42, 6391–6398, https://doi.org/10.1002/2015GL064590, 2015.

Bean, C. J. and Vogfjörd, K. S.: Seismic array data for monitoring and tracking tremor sources during subglacial floods and volcanic eruptions at Vatnajökull (Vatna Glacier), Iceland, https://doi.org/10.14470/0Y7568667884, 2020.

Behm, M., Walter, J. I., Binder, D., Cheng, F., Citterio, M., Kulessa, B., Langley, K., Limpach, P., Mertl, S., Schöner, W., Tamstorf, M., and Weyss, G.: Seismic characterization of a rapidly-rising jökulhlaup cycle at the A.P. Olsen Ice Cap, NE-Greenland, Journal of Glaciology, 66, 329–347, https://doi.org/10.1017/jog.2020.9, 2020.

Benediktsdóttir, Á., Gudmundsson, Ó., Li, K. L., and Brandsdóttir, B.: Volcanic tremor of the 2010 Eyjafjallajökull eruption, Geophysical Journal International, 228, 1015–1037, https://doi.org/10.1093/gji/ggab378, 2021.

Beyreuther, M., Barsch, R., Krischer, L., Megies, T., Behr, Y., and Wassermann, J.: ObsPy: A Python Toolbox for Seismology, Seismological Research Letters, 81, 530–533, https://doi.org/10.1785/gssrl.81.3.530, 2010.

Björnsson, H.: Marginal and supraglacial lakes in Iceland, Jökull, 26, 40–51, 1976.

Björnsson, H.: The cause of jökulhlaups in the Skaftá River, Vatnajökull, Jökull, 27, 71–78, 1977.

Björnsson, H.: Surface and bedrock topography of ice caps in Iceland, mapped by radio echo-sounding, Annals of Glaciology, 8, 11–18, 1986.

Björnsson, H.: Hydrology of Ice Caps in Volcanic Regions, Vísindafélag Íslendinga, 45, 139pp., 21 maps, 1988.

Björnsson, H.: Jökulhlaups in Iceland: prediction, characteristics and simulation, Annals of Glaciology, 16, 95–106, https://doi.org/10.3198/1992AoG16-1-95-106, 1992.

Björnsson, H.: Subglacial lakes and jökulhlaups in Iceland, Global and Planetary Change, 35, 255–271, https://doi.org/10.1016/S0921-8181(02)00130-3, 2003.

Björnsson, H.: Understanding jökulhlaups: from tale to theory, Journal Of Glaciology, 56, 1002–1010, https://doi.org/doi:10.3189/002214311796406086, 2010.

Böðvarsson, R. and Lund, B.: The SIL seismological data acquisition system —As operated in Iceland and in Sweden—, in: Methods and Applications of Signal Processing in Seismic Network Operations, pp. 131–148, Springer Berlin Heidelberg, Berlin, Heidelberg, https://doi.org/10.1007/BFb0117700, 2003.

Böðvarsson, R., Rögnvaldsson, S. T., Jakobsdóttir, S. S., Slunga, R., and Stefánsson, R.: The SIL Data Acquisition and Monitoring System, Seismological Research Letters, 67, 35–46, https://doi.org/10.1785/gssrl.67.5.35, 1996.

Böðvarsson, R., Rögnvaldsson, S. T., Slunga, R., and Kjartansson, E.: The SIL data acquisition system-at present and beyond year 2000, Physics of the Earth and Planetary Interiors, 113, 89–101, https://doi.org/10.1016/S0031-9201(99)00032-1, 1999.

Burtin, A., Bollinger, L., Vergne, J., Cattin, R., and Nábělek, J. L.: Spectral analysis of seismic noise induced by rivers: A new tool to monitor spatiotemporal changes in stream hydrodynamics, Journal of Geophysical Research: Solid Earth, 113, 1–14, https://doi.org/10.1029/2007JB005034, 2008.

https://doi.org/10.5194/egusphere-2022-644
Preprint. Discussion started: 20 July 2022

Burtin, A., Cattin, R., Bollinger, L., Vergne, J., Steer, P., Robert, A., Findling, N., and Tiberi, C.: Towards the hydrologic and bed load monitoring from high-frequency seismic noise in a braided river: The "torrent de St Pierre", French Alps, Journal of Hydrology, 408, 43–53, https://doi.org/10.1016/j.jhydrol.2011.07.014, 2011.

Capon, J.: High-resolution frequency-wavenumber spectrum analysis, Adaptive Antennas for Wireless Communications, 57, 146–156, https://doi.org/10.1109/9780470544075.ch2, 2009.

Chapp, E., Bohnenstiehl, D. R., and Tolstoy, M.: Sound-channel observations of ice-generated tremor in the Indian Ocean, Geochemistry, Geophysics, Geosystems, 6, Q06 003, https://doi.org/10.1029/2004GC000889, 2005.

Cook, K. L., Andermann, C., Gimbert, F., Adhikari, B. R., and Hovius, N.: Glacial lake outburst floods as drivers of fluvial erosion in the Himalaya, Science, 362, 53–57, 2018.

Driedger, C. L. and Fountain, A. G.: Glacier outburst floods at Mount Rainier, Washington State, USA, Annals of Glaciology, 13, 51–55, 1989.

Eibl, E. P., Bean, C. J., Jónsdóttir, I., Höskuldsson, A., Thordarson, T., Coppola, D., Witt, T., and Walter, T. R.: Multiple coincident eruptive seismic tremor sources during the 2014-2015 eruption at Holuhraun, Iceland, Journal of Geophysical Research: Solid Earth, 122, 2972–2987, https://doi.org/10.1002/2016JB013892, 2017a.

Eibl, E. P., Bean, C. J., Vogfjörd, K. S., Ying, Y., Lokmer, I., Möllhoff, M., O'Brien, G. S., and Pálsson, F.: Tremor-rich shallow dyke formation followed by silent magma flow at Bárdarbunga in Iceland, Nature Geoscience, 10, 299–304, https://doi.org/10.1038/ngeo2906, 2017b.

Eibl, E. P., Bean, C. J., Einarsson, B., Pàlsson, F., and Vogfjörd, K. S.: Seismic ground vibrations give advanced early-warning of subglacial floods, Nature Communications, 11, https://doi.org/10.1038/s41467-020-15744-5, 2020.

Einarsson, B.: Jökulhlaups in Skaftá: A study of a jökulhlaup from the Western Skaftá cauldron in the Vatnajökull ice cap, Iceland, Ph.D. thesis, 2009.

Einarsson, B., Magnússon, E., Roberts, M. J., Pálsson, F., Thorsteinsson, T., and Jóhannesson, T.: A spectrum of jökulhlaup dynamics revealed by GPS measurements of glacier surface motion, Annals of Glaciology, 57, 47–61, https://doi.org/10.1017/aog.2016.8, 2016.

Einarsson, B., Jóhannesson, T., Thorsteinsson, T., Gaidos, E., and Zwinger, T.: Subglacial flood path development during a rapidly rising jökulhlaup from the western Skaftá cauldron, Vatnajökull, Iceland, Journal of Glaciology, 63, 670–682, https://doi.org/10.1017/jog.2017.33, 2017.

Fahnestock, M., Abdalati, W., Joughin, I., Brozena, J., and Gogineni, P.: High Geothermal Heat Flow, Basal Melt, and the Origin of Rapid Ice Flow in Central Greenland, Science, 294, 2338–2342, https://doi.org/10.1126/science.1065370, 2001.

Galeczka, I., Eiriksdottir, E. S., Hardardottir, J., Oelkers, E. H., Torssander, P., and Gislason, S. R.: The effect of the 2002 glacial flood on dissolved and suspended chemical fluxes in the Skaftá river, Iceland, Journal of Volcanology and Geothermal Research, 301, 253–276, https://doi.org/10.1016/j.jvolgeores.2015.05.008, 2015.

Gimbert, F., Tsai, V. C., and Lamb, M. P.: Journal of Geophysical Research : Earth Surface A physical model for seismic noise generation by turbulent flow in rivers, Journal of Geophysical Research: Earth Surface, 119, 2209–2238, https://doi.org/10.1002/2014JF003201.Received, 2014.

Gimbert, F., Tsai, V. C., Amundson, J. M., Bartholomaus, T. C., and Walter, J. I.: Subseasonal changes observed in subglacial channel pressure, size, and sediment transport, Geophysical Research Letters, 43, 3786–3794, https://doi.org/10.1002/2016GL068337, 2016.

Grinsted, A., Hvidberg, C. S., Campos, N., and Dahl-Jensen, D.: Periodic outburst floods from an ice-dammed lake in East Greenland, Scientific Reports, 7, 7–12, https://doi.org/10.1038/s41598-017-07960-9, 2017.

https://doi.org/10.5194/egusphere-2022-644
Preprint. Discussion started: 20 July 2022

Gudmundsson, M. T. and Björnsson, H.: Eruptions in Grímsvötn, Vatnajökull, Iceland, 1934–1991, Jökull, 41, 21–45, 1991.

Gudmundsson, M. T., Sigmundsson, F., and Björnsson, H.: Ice–volcano interaction of the 1996 Gjalp subglacial eruption, Vatnajökull, Iceland, Nature, 389, 954–957, https://doi.org/10.1038/40122, 1997.

Heeszel, D. S., Walter, F., and Kilb, D. L.: Humming glaciers, Geology, 42, 1099–1102, https://doi.org/10.1130/G35994.1, 2014.

Herring, T. A., King, R. W., Mcclusky, S. C., and Sciences, P.: Introduction to GAMIT / GLOBK, Tech. Rep. June 2015, Mass. Instit. Tech., http://www-gpsg.mit.edu/$\sim$simon/gtgk, 2015.

Hsu, L., Finnegan, N. J., and Brodsky, E. E.: A seismic signature of river bedload transport during storm events, Geophysical Research Letters, 38, 1–6, https://doi.org/10.1029/2011GL047759, 2011.

Jóhannesson, T.: Propagation of a subglacial flood wave during the initiation of a jökulhlaup, Hydrological Sciences Journal, 47, 417–434, https://doi.org/10.1080/02626660209492944, 2002.

Jóhannesson, T., Thorsteinsson, T., Stefánsson, A., Gaidos, E. J., and Einarsson, B.: Circulation and thermodynamics in a subglacial geothermal lake under the Western Skaftá cauldron of the Vatnajökull ice cap, Iceland, Geophysical Research Letters, 34, 1–6, https://doi.org/10.1029/2007GL030686, 2007.

Jones, M. T., Gałeczka, I. M., Gkritzalis-Papadopoulos, A., Palmer, M. R., Mowlem, M. C., Vogfjörd, K., Jónsson, T., and Gislason, S. R.: Monitoring of jökulhlaups and element fluxes in proglacial Icelandic rivers using osmotic samplers, Journal of Volcanology and Geothermal Research, 291, 112–124, https://doi.org/10.1016/j.jvolgeores.2014.12.018, 2015.

Krueger, F. and Weber, M.: The effect of low-velocity sediments on the mislocation vectors of the GRF array, Geophysical Journal International, 108, 387–393, https://doi.org/10.1111/j.1365-246X.1992.tb00866.x, 1992.

Leet, R. C.: Saturated and subcooled hydrothermal boiling in groundwater flow channels as a source of harmonic tremor, Journal of Geophysical Research, 93, 4835, https://doi.org/10.1029/JB093iB05p04835, 1988.

Lindner, F., Walter, F., Laske, G., and Gimbert, F.: Glaciohydraulic seismic tremors on an Alpine glacier, The Cryosphere Discussions, 15, 12–19, https://doi.org/10.3929/ethz-a-010782581, 2020.

Lipovsky, B. P. and Dunham, E. M.: Tremor during ice-stream stick slip, Cryosphere, 10, 385–399, https://doi.org/10.5194/tc-10-385-2016, 2016.

Livingstone, S. J., Sole, A. J., Storrar, R. D., Harrison, D., Ross, N., and Bowling, J.: Brief Communication : Outburst floods triggered by periodic drainage of subglacial lakes , Isunguata Sermia , West Greenland, The Cryosphere Discussions, 2019.

Loose, B., Naveira Garabato, A. C., Schlosser, P., Jenkins, W. J., Vaughan, D., and Heywood, K. J.: Evidence of an active volcanic heat source beneath the Pine Island Glacier, Nature Communications, 9, 1–9, https://doi.org/10.1038/s41467-018-04421-3, 2018.

MacAyeal, D. R., Okal, E. A., Aster, R. C., and Bassis, J. N.: Seismic and hydroacoustic tremor generated by colliding Icebergs, Journal of Geophysical Research: Earth Surface, 113, 1–10, https://doi.org/10.1029/2008JF001005, 2008.

Magnússon, E., Rott, H., Björnsson, H., and Pálsson, F.: The impact of jökulhlaups on basal sliding observed by SAR interferometry on Vatnajökull, Iceland, Journal of Glaciology, 53, 232–240, https://doi.org/10.3189/172756507782202810, 2007.

Magnússon, E., Gudmundsson, M. T., Roberts, M. J., Sigurdsson, G., Höskuldsson, F., and Oddsson, B.: Ice-volcano interactions during the 2010 Eyjafjallajkull eruption, as revealed by airborne imaging radar, Journal of Geophysical Research: Solid Earth, 117, 1–17, https://doi.org/10.1029/2012JB009250, 2012.

Megies, T., Beyreuther, M., Barsch, R., Krischer, L., and Wassermann, J.: ObsPy - what can it do for data centers and observatories?, Annals of Geophysics, 54, 47–58, https://doi.org/10.4401/ag-4838, 2011.

https://doi.org/10.5194/egusphere-2022-644
Preprint. Discussion started: 20 July 2022

Montanaro, C., Scheu, B., Gudmundsson, M. T., Vogfjörd, K., Reynolds, H. I., Dürig, T., Strehlow, K., Rott, S., Reuschlé, T., and Dingwell, D. B.: Multidisciplinary constraints of hydrothermal explosions based on the 2013 Gengissig lake events, Kverkfjöll volcano, Iceland, Earth and Planetary Science Letters, 434, 308–319, https://doi.org/10.1016/j.epsl.2015.11.043, 2016.

Müller, C., Schlindwein, V., Eckstaller, A., and Miller, H.: Geophysics: Singing icebergs, Science, 310, 1299, https://doi.org/10.1126/science.1117145, 2005.

Old, G. H., Lawler, D. M., and Snorrason, Á.: Discharge and suspended sediment dynamics during two jökulhlaups in the Skaftá river, Iceland, Earth Surface Processes and Landforms, 30, 1441–1460, https://doi.org/10.1002/esp.1216, 2005.

Pálsson, F., Gunnarsson, A., Jónsson, , Steinþórsson, S., and Pálsson, H. S.: Vatnajökull: Mass blance, meltwater drainage and surface velocity of theglacial year 2012-2013, Tech. rep., Institute of Earth Sciences University of Iceland and National Power Company. RH-14-2016, 2014.

Podolskiy, E. A. and Walter, F.: Cryoseismology, Reviews of Geophysics, 54, 708–758, https://doi.org/10.1002/2016RG000526, 2016.

Richardson, D.: Glacier outburst floods in the Pacific northwest, vol. V.S. Geol., 1968.

Roberts, M. J.: Jökulhlaups: A reassessment of floodwater flow through glaciers, Reviews of Geophysics, 43, 1–21, https://doi.org/10.1029/2003RG000147, 2005.

Roberts, M. J., Stefánsson, R., Björnsson, H., Russell, A. J., Tweed, F. S., Harris, T. D., Fay, H., Knudsen, Ó., and Guðmundsson, G. B.: Recent jökulhlaups from Western Vatnajökull, Iceland: Hydrologic insights from seismic tremor measurements and aerial observations, in: EGS-AGU-EUG Joint Assembly, 2003.

Roberts, M. J., Pálsson, F., Gudmundsson, M. T., Björnsson, H., and Tweed, F. S.: Ice–water interactions during floods from Grænalón glacier-dammed lake, Iceland, Annals of Glaciology, 40, 133–138, https://doi.org/10.3189/172756405781813771, 2005.

Rögnvaldsson, S. and Slunga, R.: Routine Fault Plane Solutions for Local Networks: a Test With Synthetic Data, Bulletin of the Seismological Society of America, 83, 1232–1247, 1993.

Röösli, C., Walter, F., Husen, S., Andrews, L. C., Lüthi, M. P., Catania, G. A., and Kissling, E.: Sustained seismic tremors and icequakes detected in the ablation zone of the Greenland ice sheet, Journal of Glaciology, 60, 563–575, https://doi.org/10.3189/2014joG13j210, 2014.

Röösli, C., Walter, F., Ampuero, J. P., and Kissling, E.: Seismic moulin tremor, Journal of Geophysical Research: Solid Earth, 121, 5838–5858, https://doi.org/10.1002/2015JB012786, 2016.

Schmandt, B., Aster, R. C., Scherler, D., Tsai, V. C., and Karlstrom, K.: Multiple fluvial processes detected by riverside seismic and infrasound monitoring of a controlled flood in the Grand Canyon, Geophysical Research Letters, 40, 4858–4863, https://doi.org/10.1002/grl.50953, 2013.

Schroeder, D. M., Blankenship, D. D., Young, D. A., and Quartini, E.: Evidence for elevated and spatially variable geothermal flux beneath the West Antarctic Ice Sheet, Proceedings of the National Academy of Sciences of the United States of America, 111, 9070–9072, https://doi.org/10.1073/pnas.1405184111, 2014.

Schweitzer, J.: Slowness corrections - One way to improve IDC products, Pure and Applied Geophysics, 158, 375–396, https://doi.org/10.1007/PL00001165, 2001.

Sigmundsson, F., Hooper, A., Hreinsdóttir, S., Vogfjörd, K. S., Ófeigsson, B. G., Heimisson, E. R., Dumont, S., Parks, M., Spaans, K., Gudmundsson, G. B., Drouin, V., Árnadóttir, T., Jónsdóttir, K., Gudmundsson, M. T., Högnadóttir, T., Fridriksdóttir, H. M., Hensch, M., Einarsson, P., Magnússon, E., Samsonov, S., Brandsdóttir, B., White, R. S., Ágústsdóttir, T., Greenfield, T., Green, R. G., Hjartardóttir, Á. R., Pedersen, R., Bennett, R. A., Geirsson, H., la Femina, P. C., Björnsson, H., Pálsson, F., Sturkell, E., Bean, C. J., Möllhoff, M.,

https://doi.org/10.5194/egusphere-2022-644
Preprint. Discussion started: 20 July 2022

Braiden, A. K., and Eibl, E. P.: Segmented lateral dyke growth in a rifting event at Bárðarbunga volcanic system, Iceland, Nature, 517, 191–195, https://doi.org/10.1038/nature14111, 2014.

Stefansson, R., Bodvarsson, R., Slunga, R., Einarsson, P., Jakobsdottir, S., Bungum, H., Gregersen, S., Havskov, J., Hjelme, J., and Korhonen, H.: Earthquake prediction research in the South Iceland Seismic Zone and the SIL Project, Bulletin of the Seismological Society of America, 83, 696–716, 1993.

Sturkell, E., Einarsson, P., Roberts, M. J., Geirsson, H., Gudmundsson, M. T., Sigmundsson, F., Pinel, V., Gudmundsson, G. B., Ólafsson, H., and Stefánsson, R.: Seismic and geodetic insights into magma accumulation at Katla subglacial volcano, Iceland: 1999 to 2005, Journal of Geophysical Research: Solid Earth, 113, 1–17, https://doi.org/10.1029/2006JB004851, 2008.

Tómasson, H. and Vilmundardóttir, E. G.: Nokkrar athuganir við Langasjó [Several observations at lake Langasjór], National Energy Authority, report 10385, 1967.

Vogfjörd, K. and Langston, C.: Characteristics of short-period wave propagation in regions of Fennoscandia, with emphasis on Lg, Bulletin of the Seismological Society of America, 86, 1873–1895, 1996.

Vore, M. E., Bartholomaus, T. C., Winberry, J. P., Walter, J. I., and Amundson, J. M.: Seismic Tremor Reveals Spatial Organization and Temporal Changes of Subglacial Water System, Journal of Geophysical Research: Earth Surface, 124, 1–20, https://doi.org/10.1029/2018jf004819, 2019.

Wagner, W., Cooper, J. R., Dittmann, A., Kijima, J., Kretzschmar, H.-J., Kruse, A., Mares, R., Oguchi, K., Sato, H., Stöcker, I., Sifner, O., Takaishi, Y., Tanishita, I., Trübenbach, J., and Willkommen, T.: The IAPWS Industrial Formulation 1997 for the Thermodynamic Properties of Water and Steam, Tech. Rep. 1, Erlangen, Germany, https://doi.org/10.1115/1.483186, 2000.

Waythomas, C. F., Pierson, T. C., Major, J. J., and Scott, W. E.: Voluminous ice-rich and water-rich lahars generated during the 2009 eruption of Redoubt Volcano, Alaska, Journal of Volcanology and Geothermal Research, 259, 389–413, https://doi.org/10.1016/j.jvolgeores.2012.05.012, 2013.

Werder, M. A. and Funk, M.: Dye tracing a jökulhlaup: II. Testing a jökulhlaup model against flow speeds inferred from measurements, Journal of Glaciology, 55, 899–908, https://doi.org/10.3189/002214309790152375, 2009.

Winberry, J. P., Anandakrishnan, S., and Alley, R. B.: Seismic observations of transient subglacial water-flow beneath MacAyeal Ice Stream, West Antarctica, Geophysical Research Letters, 36, L11 502, https://doi.org/10.1029/2009GL037730, 2009.

Winberry, J. P., Anandakrishnan, S., Wiens, D. A., and Alley, R. B.: Nucleation and seismic tremor associated with the glacial earthquakes of Whillans Ice Stream, Antarctica, Geophysical Research Letters, 40, 312–315, https://doi.org/10.1002/grl.50130, 2013.

Ying, Y., Eibl, E. P. S., Bean, C. J., Vogfjörd, K., and Pálsson, F.: Full Wavefield Numerical Simulations of Sub-glacial Seismic Tremor at Vatnajökull Glacier, Iceland, in: EGU General Assembly Conference Abstracts, vol. 17, 2015.

Zóphóníasson, S.: Rennsli í Skaftárhlaupum 1955-2002, Tech. rep., Reykjavík, National Energy Authority, Report SZ-2002/01, 2002.

Þórarinsson, S. and Rist, S.: Skaftárhlaup í september 1955 [Jökulhlaup in Skaftá in September 1955], Jökull, 5, 37–40, 1955.

https://doi.org/10.5194/egusphere-2022-644
Preprint. Discussion started: 20 July 2022

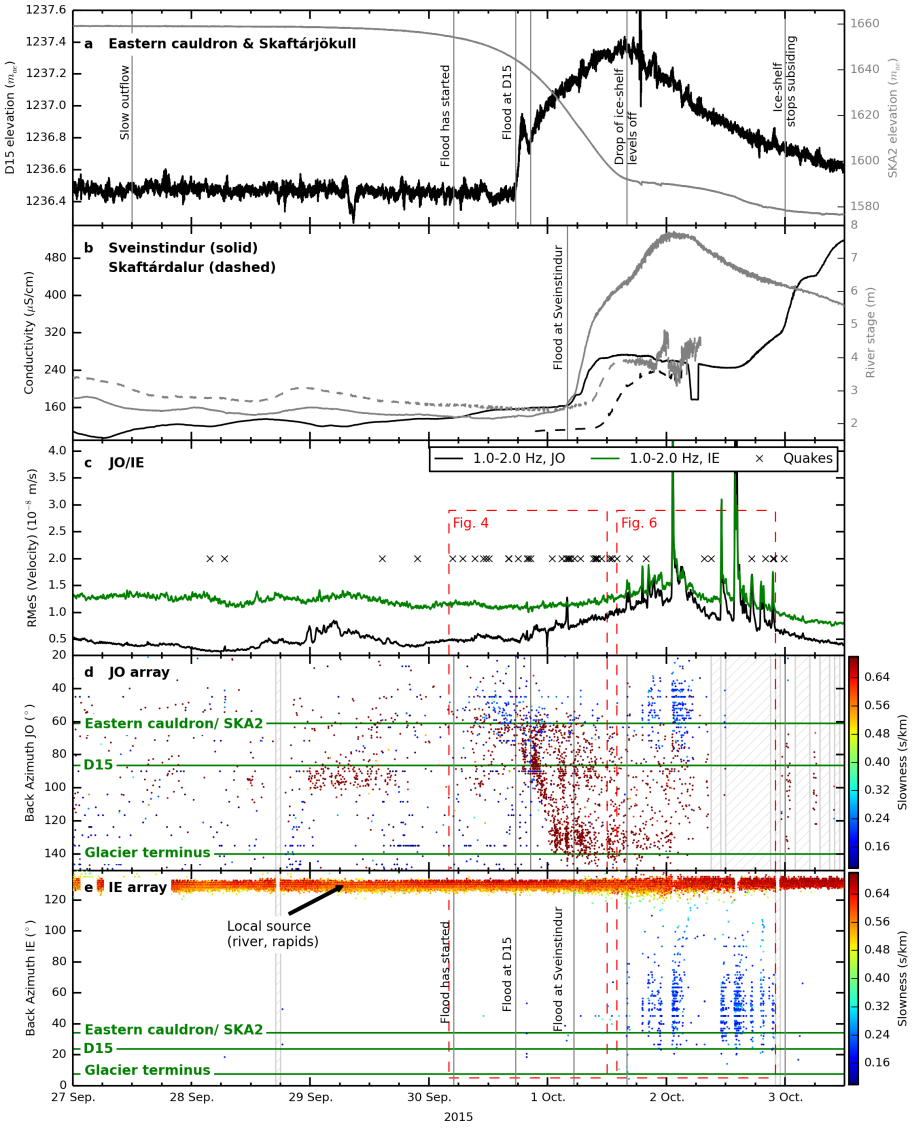

Figure 3. The flood in September/October 2015 is detected by GPS sensors, hydrological stations, seismic arrays and the SIL network (for station locations see Fig. 1). Gray lines mark important events during the flood, detected by various instruments for comparison with the tremor. (a) The elevation of GPS instruments in the eastern cauldron (SKA2) and on Skaftárjökull (D15) above the GRS80/WGS84 ellipsoid (67.23 m at D15 and 67.72 m at SKA2). (b) River stage (gray) and conductivity (black) of Skaftá river measured at Sveinstindur (solid) and in Skaftárdalur (dashed). (c) Root Median Square (RMeS) of the seismic amplitude filtered 1 to 2 Hz at JO and IE arrays. The occurrence times of located quakes (Fig. 1) are marked with black ×-signs. (d) Dots indicate the dominant back azimuth in each 18 s long time window at JO array filtered between 1.2 and 2.6 Hz colored according to slowness. The green horizontal lines respectively mark the back azimuth of signals from the eastern Skaftá cauldron, D15 and the point where the Skaftá river emerges from under the glacier. (e) Same as d but for IE array. The y-axis is reversed to ease comparison with subfigure d.

https://doi.org/10.5194/egusphere-2022-644
Preprint. Discussion started: 20 July 2022

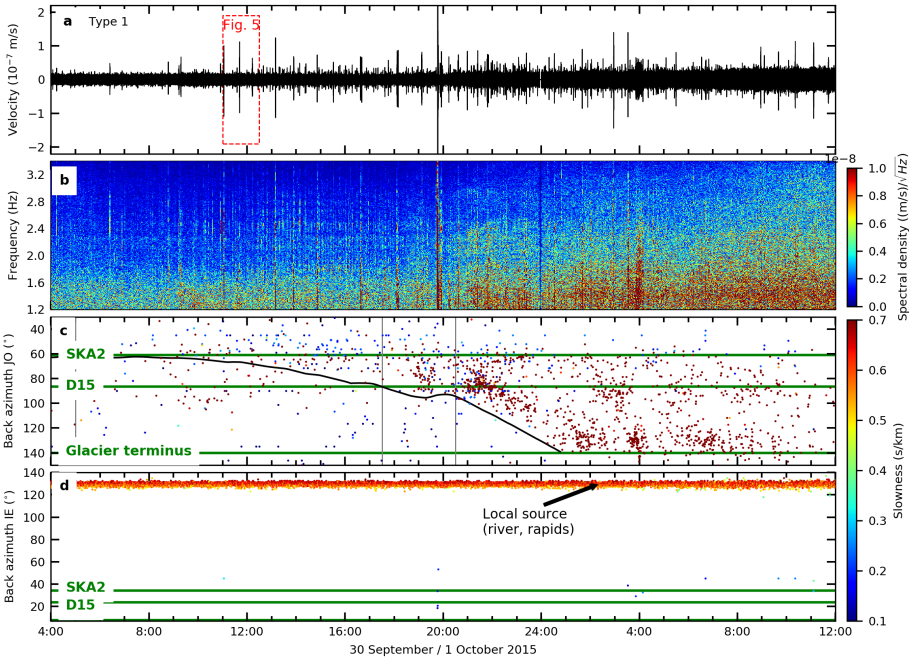

Figure 4. Subglacial Type 1 tremor followed the migrating flood front. (a) Vertical velocity seismogram from 04:00 on 30 September to 12:00 on 1 October 2015 filtered between 1.2 and 3.4 Hz. Some of the 'spikes' in subfigures a and b are not part of the tremor but short quakes from the cauldron area or earthquakes in other nearby locations like Bárðarbunga volcano (see Fig. 5). (b) Amplitude spectrogram made with a fast Fourier transform window length of 256 s and 50% overlap. (c) Dots indicate the dominating back azimuth at JO array in each 18 s long time window colored according to slowness. Green horizontal lines as in Fig. 1 and 3. Grey vertical lines as in Fig. 3. The black curve shows changes in back azimuth at JO corresponding to a point migrating along the flood path (Fig. 2) with a constant velocity 2 km/h passing D15 at 17:30 on 30 September. (d) Same as subfigure c but for IE array.

https://doi.org/10.5194/egusphere-2022-644
Preprint. Discussion started: 20 July 2022

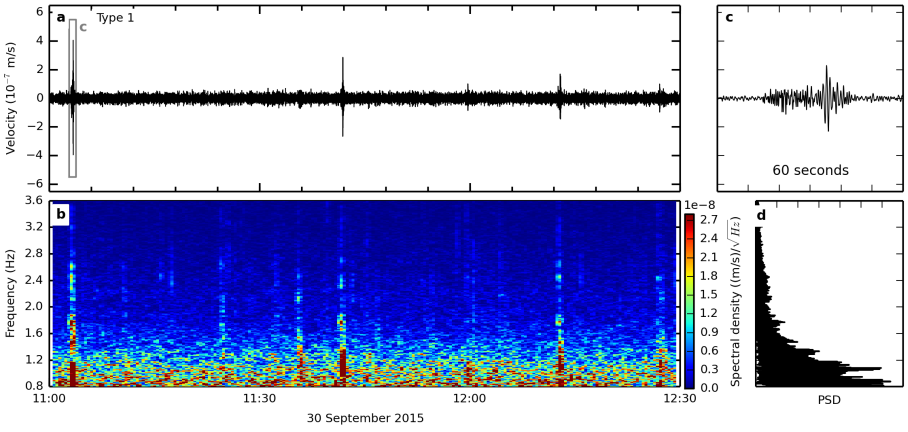

Figure 5. Quakes followed the start of the flood. (a) Seismogram between 11:00 and 12:30 on 30 September 2015 filtered between 0.8 and 3.6 Hz, (b) amplitude spectrogram made with a fast Fourier transform window length of 64 s and 70% overlap. (c) 1 minute long time window showing a discrete event filtered between 1 and 8 Hz and (d) spectrum of subfigure b.

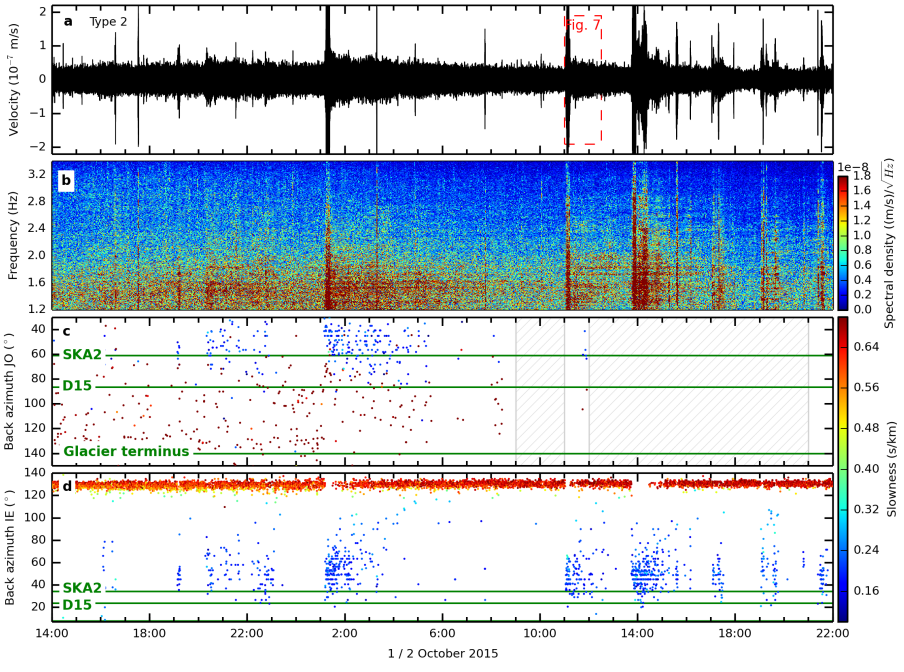

Figure 6. Type 2 tremor bursts and harmonic tails occurred after most water drained from the subglacial lake. Tremor from the cauldron area from 14:00 on 1 October to 22:00 on 2 October 2015. Subfigures as in Fig. 4.

https://doi.org/10.5194/egusphere-2022-644
Preprint. Discussion started: 20 July 2022

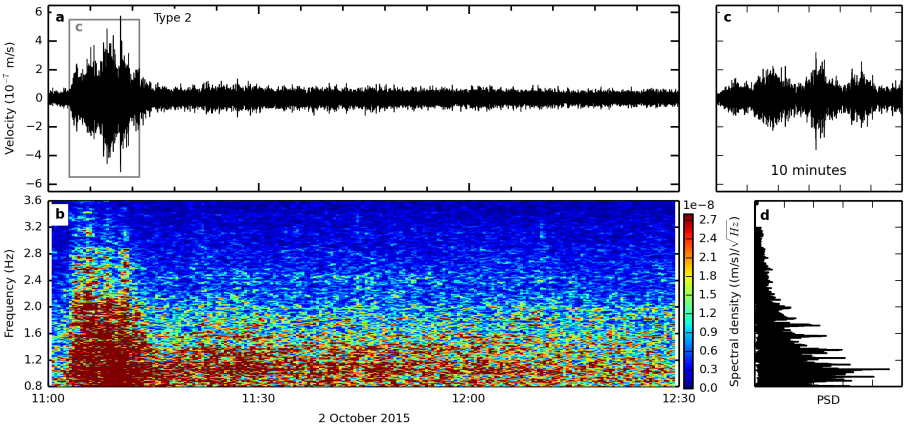

Figure 7. Zoom into one Type 2 tremor burst and its harmonic tail from 11:00 to 12:30 on 2 October 2015. Subfigures a, b and d as in Fig. 5 but in (b) with a fast Fourier transform window length of 84 s. (c) 10 minutes long time window showing a tremor burst filtered between 1.2 and 3.6 Hz.

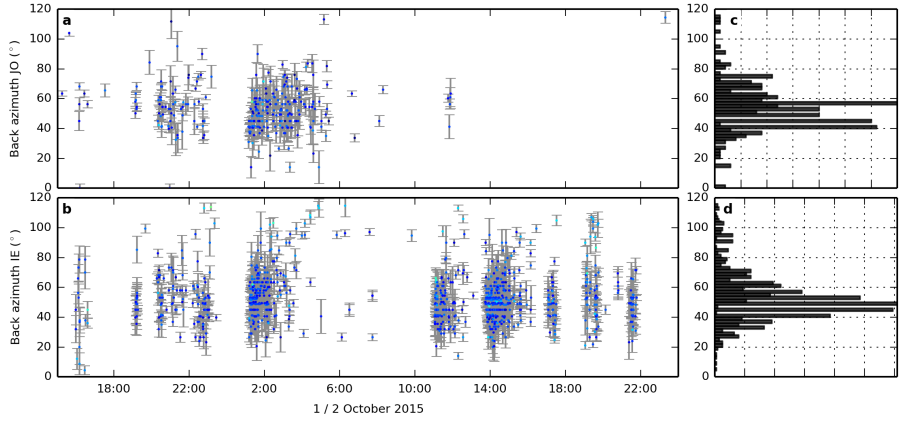

Figure 8. Back azimuths associated with the Type 2 tremor bursts at (a) JO and (b) IE array. Histograms illustrate the dominant back azimuths at (c) JO and (d) IE array that indicate a source in the cauldron area.